

STRUCTURE OF THE X-RAY EMISSION FROM THE JET OF 3C 273

H. L. MARSHALL,¹ D. E. HARRIS,² J. P. GRIMES,² J. J. DRAKE,² A. FRUSCIONE,² M. JUDA,² R. P. KRAFT,² S. MATHUR,³
S. S. MURRAY,² P. M. OGLE,¹ D. O. PEASE,² D. A. SCHWARTZ,² A. L. SIEMIGINOWSKA,² S. D. VRTILEK,² AND B. J. WARGELIN²

Received 2000 September 11; accepted 2000 December 6; published 2001 February 000

ABSTRACT

We present images from five observations of the quasar 3C 273 with the *Chandra X-Ray Observatory*. The jet has at least four distinct features that are not resolved in previous observations. The first knot in the jet (A1) is very bright in X-rays. Its X-ray spectrum is well fitted with a power law with $\alpha = 0.60 \pm 0.05$ (where $S_\nu \propto \nu^{-\alpha}$). Combining this measurement with lower frequency data shows that a pure synchrotron model can fit the spectrum of this knot from 1.647 GHz to 5 keV (over nine decades in energy) with $\alpha = 0.76 \pm 0.02$, similar to the X-ray spectral slope. Thus, we place a lower limit on the total power radiated by this knot of 1.5×10^{43} ergs s^{-1} ; substantially more power may be emitted in the hard X-ray and γ -ray bands. Knot A2 is also detected and is somewhat blended with knot B1. Synchrotron emission may also explain the X-ray emission, but a spectral bend is required near the optical band. For knots A1 and B1, the X-ray flux dominates the emitted energy. For the remaining optical knots (C through H), localized X-ray enhancements that might correspond to the optical features are not clearly resolved. The position angle of the jet ridge line follows the optical shape with distinct, aperiodic excursions of $\pm 1^\circ$ from a median value of -138° . Finally, we find X-ray emission from the “inner jet” between $5''$ and $10''$ from the core.

Subject headings: galaxies: jets — quasars: individual (3C 273) — X-rays: galaxies

1. INTRODUCTION

Previous high-resolution observations of the 3C 273 jet using MERLIN at 1.647 GHz and the *Hubble Space Telescope (HST)* Wide Field Planetary Camera 2 (Bahcall et al. 1995) showed that the overall shape of the jet is somewhat different between the optical and radio bands. The optical image appears dominated by elongated knots roughly $0''.1$ by $0''.5$ in size, while the radio image gives an indication of a “cocoon” structure, especially at the end, or “head.” Bahcall et al. speculated that the cocoon is slowly moving material enveloping a relativistically moving flow. Although relativistic motion is required to explain superluminal motion in the quasar core, it is not yet clear that the flow is relativistic in the jet on a kiloparsec scale.

Harris & Stern (1987) used the *Einstein Observatory* data on 3C 273 to detect X-ray emission from the jet, which was less than 1% of the flux of the core. More recently, Röser et al. (2000) examined *ROSAT* HRI images at $\sim 5''$ resolution to show that the X-ray emission drops with distance along the jet. Using models of the profile along the jet and multicolor ground-based images at $1''.3$ resolution, they generated spectral energy distributions (SEDs) for knots in the jet and found that the X-ray flux of knot A1⁴ is consistent with that expected by extrapolating a simple synchrotron model from the radio through the optical with one population of electrons. The highest energy electrons in their model had $\gamma > 10^7$. Synchrotron self-Compton (SSC) calculations generally fail to predict X-ray intensities commensurate with those observed for any of the knots.

X-ray images from the *Chandra X-Ray Observatory* are now resolving the spatial structure along quasar jets. The first such image, of the quasar PKS 0637–752, proved remarkable be-

cause of the strong X-ray fluxes of the jet knots, relative to the radio fluxes (Schwartz et al. 2000). Simple synchrotron and thermal models could be ruled out easily, while SSC models required unreasonable conditions. Tavecchio et al. (2000) and Celotti, Ghisellini, & Chiaberge (2001) have suggested that inverse Compton scattering of the cosmic microwave background could produce the required X-ray fluxes and require the jet material to be moving relativistically at a small angle to the line of sight as in models of the core. We present *Chandra* images and spectra for the jet in 3C 273 that we examine in light of these models.

2. OBSERVATIONS AND ANALYSIS

2.1. X-Ray Data Reduction

3C 273 was observed three times as part of the calibration of the *Chandra* grating spectrometers, once in a direct imaging mode as part of science verification and twice more as the gratings failed to insert during calibration observations. See Table 1 for a list of observations, totaling 193,230 s of exposure time. Results from the dispersed spectra of the core are still being analyzed as part of the ongoing effort to verify the grating spectrometer effective area calibration and will be presented elsewhere. The Low Energy Transmission Grating (LETG) and High Resolution Camera (HRC) combination gave significantly fewer counts in the jet compared with the others and so was not used in the combined X-ray image. We present here the results from the zeroth-order portion of the ACIS grating observations and combine these data with those of the HRC-I and ACIS-S imaging observations for image analysis. The dispersed spectra of the jet were extremely faint; we determined that there were no significant emission lines and did not examine these data any further.

Each of the grating observations had well-known artifacts that distort the zeroth-order images. Two artifacts are relevant to observations of the jet. Bright sources observed with ACIS will show up with a “readout streak” (see the *Chandra* Proposers’ Observatory Guide [POG]). In no ACIS observation,

¹ Center for Space Research, Massachusetts Institute of Technology, 70 Vassar Street, Cambridge, MA 02139; hermann@space.mit.edu.

² Harvard-Smithsonian Center for Astrophysics, 60 Garden Street, Cambridge, MA 02138.

³ Ohio State University.

⁴ We will refer to the knot-naming convention given by Bahcall et al. (1995; reproduced in Fig. 1).

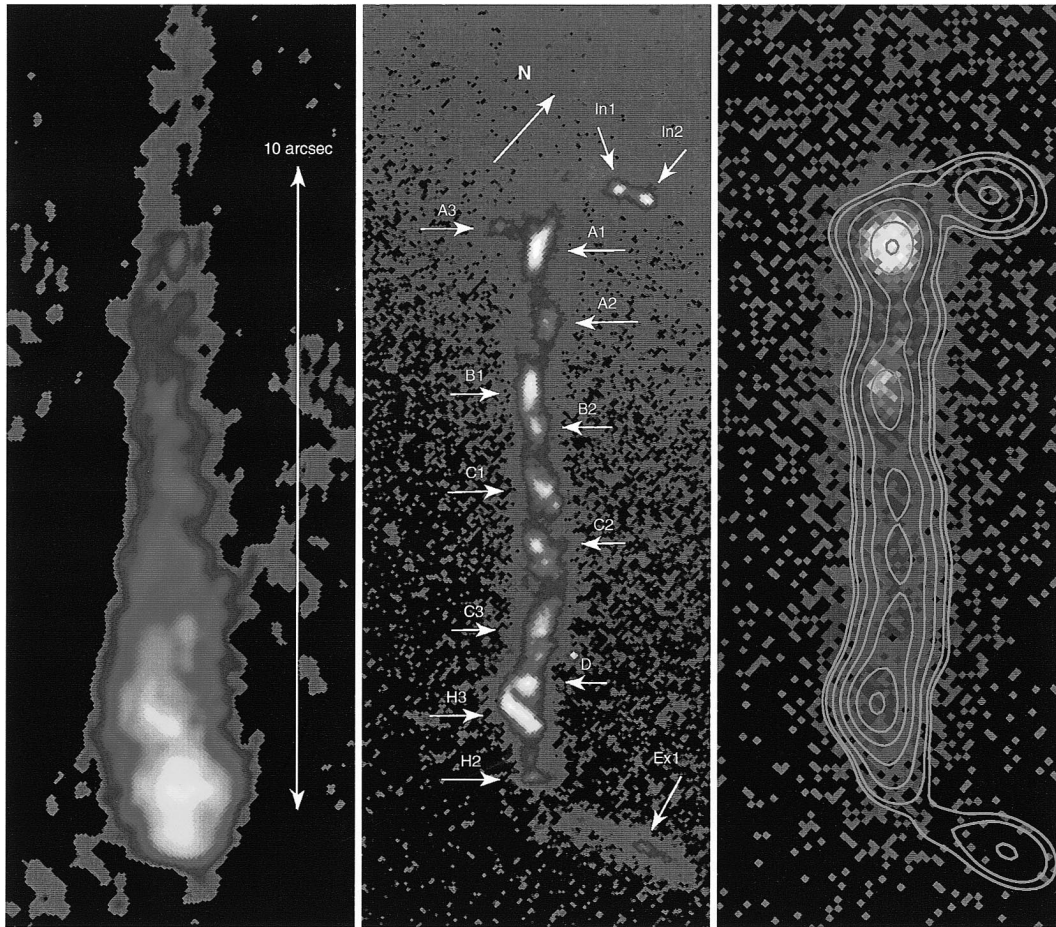


FIG. 1.—Images of the jet in 3C 273 in three different bands. *Left*: Image at 1.647 GHz using the MERLIN array, kindly provided by Tom Muxlow of Jodrell Bank. *Middle*: *Hubble Space Telescope* Planetary Camera image in the F622W filter (centered at 6170 Å). Features are labeled according to the nomenclature used by Bahcall et al. (1995). *Right*: Raw *Chandra* image of the X-ray emission from the jet of 3C 273 in 0".1 bins overlaid with a version of the *HST* image smoothed with a Gaussian profile in order to match the X-ray imaging resolution. The X-ray and optical images have been registered to each other to about 0".05 using the position of knot A1. The overall shape of the jet is remarkably similar in length and curvature, but the X-ray emission fades to the end of the jet, so individual C knots are not discernible. Other differences are more apparent in Fig. 2. The radio emission is much fainter at knot A1 and is displayed with a logarithmic scaling.

however, did the streak affect the image of the jet. The LETG has two support structures that produce diffraction patterns (see the POG). This pattern is spaced at 60° intervals and, again, did not interfere with the image of the jet. Individual observations have slightly uncertain absolute pointing, so we repositioned each image separately. The HRC and LETG/ACIS observations were combined by referencing to the core. Because of pileup, the two nongrating ACIS observations and the High Energy Transmission Grating observations had zeroth-order images that were severely affected by pileup, so the first knot was used as a reference. We estimate that the uncertainty in this procedure gives a relative offset between the core and

the jet of less than 0".05 by examining the location of the center of the wings of the core and comparing with the position of the first knot in each data set.

Figure 1 shows the combined X-ray image binned in 0".2 pixels. The jet shows clear curvature but mostly has a one-dimensional appearance, so a profile was computed for quantitative analysis. The X-ray profile (Fig. 2) was derived by summing data in a 1".5 wide window centered on a position angle of -138.0° , which is the center line of the jet. We estimate that the correction for aperture losses is $10\% \pm 5\%$ at any location along the jet, based on using a wider extraction region. The peak of emission occurs just under 13" from the core. Fitting a Gaussian profile to it, the centroid is 12.93 ± 0.01 from the core, and the dispersion of a Gaussian is 0.33 ± 0.01 (for a FWHM of 0".78). The 2σ limit to the FWHM of this knot is 0".3, given that point sources have projected FWHMs of 0".75, which is determined from readout streak data for the core of 3C 273 and other bright point sources. The next peak in the X-ray emission is clearly extended, from 14".0 to 15" from the core, dropping more steeply on the downstream side. From 16" to 21", the X-ray emission appears somewhat devoid of distinct features but with some possible surface brightness variations; there may be an unresolved knot at 20".

TABLE 1
CHANDRA OBSERVATIONS OF 3C 273

Observation ID	Detector	Grating	Date (2000)	Exposure (s)
459	ACIS-S	HETG	Jan 10	38,600
460	HRC-I	None	Jan 22	20,260
461	HRC-S	LETG	Jan 9	40,280
1198	ACIS-S	LETG	Jan 9–10	38,160
1711	ACIS-S	None	Jun 14	28,130
1712	ACIS-I	None	Jun 14	27,800

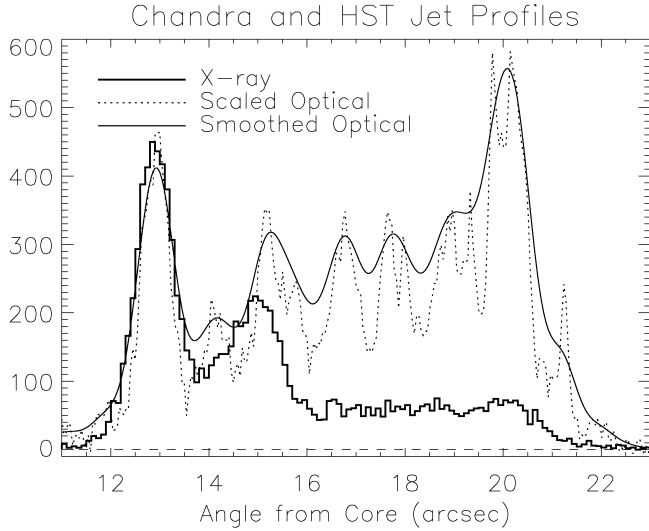


FIG. 2.—Profiles of the 3C 273 jet in the X-ray (histogram, in counts per 0.1 bin) and optical bands. The optical data are from a Planetary Camera image in filter F622W, taken from the *HST* archive, and are scaled to match the X-ray histogram for knot A1: $0.325 \mu\text{Jy}$ per 0.04554 bin at a vertical value of 500. The raw optical profile was smoothed with a Gaussian with $\sigma = 0.25$ (FWHM = 0.60) and was scaled to $0.27 \mu\text{Jy}$ per 0.04554 bin at a vertical value of 500. The optical profiles were displaced 0.22 closer to the core to provide a better match between the X-ray and optical profiles of knot A1; systematic registration uncertainties are of this order. Beyond knots A1 and B1 (12.9 and 15.0 from the core, respectively), other knots are not clearly detected individually in the X-ray profile.

The X-ray flux reaches the background level at $21''$ from the nucleus.

Several regions were selected for X-ray spectral fitting: (a) a $1''$ radius circle centered on the first bright knot, (b) a similar circle centered on the extended knot at $15''$, and (c) a rectangular box extending from $16''$ to the end of the jet. The 0.5 – 8 keV ACIS-S spectra were combined and fitted with power-law models holding N_{H} fixed at $1.71 \times 10^{20} \text{ cm}^{-2}$ (Albert et al. 1993; see Fig. 4 of this Letter). The resultant spectral indices were $\alpha_a = 0.60 \pm 0.05$, $\alpha_b = 0.88 \pm 0.07$, and $\alpha_c = 0.75 \pm 0.05$ (where $S_p \propto \nu^{-\alpha}$); no spectral evolution is detected along the jet. Flux densities of several knot regions are given in Table 2. We estimate that the total jet power is about 0.4% of the core power in the 0.5 – 5.0 keV band.

X-ray emission is just detectable between the core and the knot A1, as shown in Figure 3. The $5''$ – $10''$ annulus shows a peak at the position angle of the $10''$ – $20''$ jet in addition to peaks at the position angles of the readout streak. It is difficult to quantify precisely the flux of the inner jet because of the ripple inherent in azimuthal profiles this close to a bright source that is caused by mirror support structure. Accounting for the

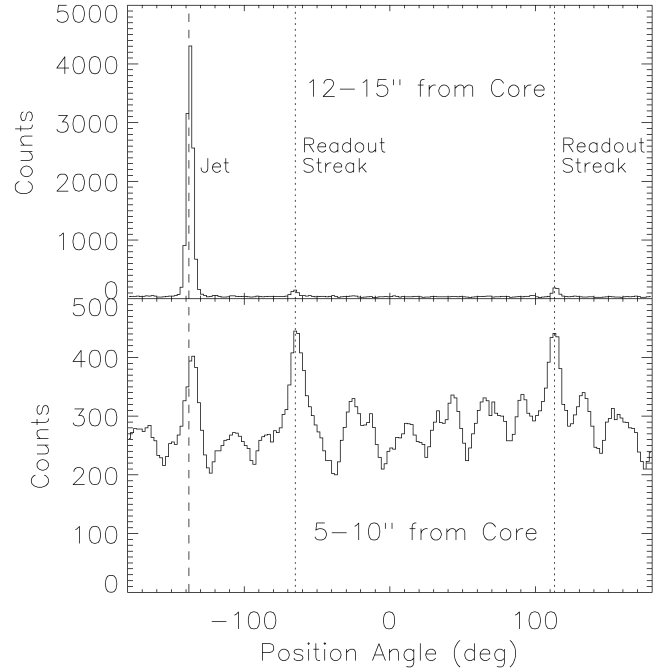


FIG. 3.—Azimuthal histograms from two different annuli centered on the quasar core. The top panel, for the annulus from $12''$ to $15''$ from the core, shows the jet at a position angle of -138° (dashed lines) and the readout streaks at about 110° and -70° (dotted lines). The bottom panel shows the histogram for the $5''$ – $10''$ annulus. The two brightest peaks are at the position angles of the readout streak, while the third brightest is at the same position angle as the large-scale jet. The ripple is due to the mirror support structure, which causes shadows every 30° . The peak at -138° is a detection of X-rays from the “inner jet,” which is not very bright optically but is detected in the radio band. The position angle of the inner jet is rotated slightly to the north compared with the $5''$ – $10''$ portion of the jet. A similar rotation is observed in the MERLIN map (see Fig. 1).

ripple by fitting a sinusoid to the local background, we estimate that the count rate from the inner jet is about 0.012 ± 0.001 counts s^{-1} , corresponding to a total flux density of 6.9 ± 0.6 nJy at 1 keV for a power-law spectrum with $\alpha = 0.6$.

2.2. Comparison with the Optical Emission

X-ray components were identified using images obtained from the *HST* archives. Fluxes were determined in filters F450W, F622W, F814W, and F160W (near-infrared camera and multiobject spectrometer).⁵ The planetary camera (PC) obser-

⁵ Based on observations made with the NASA/ESA *Hubble Space Telescope*, obtained from the data archive at the Space Telescope Science Institute. STScI is operated by the Association of Universities for Research in Astronomy, Inc., under NASA contract NAS5-26555.

TABLE 2
FLUXES OF KNOTS IN THE 3C 273 JET

Frequency (Hz)	Flux Density (μJy)		
	A1	B1	D/H3
1.65×10^9	$4.2 \pm 1.2 \times 10^4$	$4.5 \pm 2.0 \times 10^5$	$6.5 \pm 1.0 \times 10^5$
1.87×10^{14}	10.7 ± 2.3	14.8 ± 8.1	71.3 ± 10.7
3.76×10^{14}	6.7 ± 2.0	6.9 ± 1.8	13.2 ± 2.8
4.85×10^{14}	5.15 ± 0.83	5.16 ± 0.97	8.2 ± 1.2
6.59×10^{14}	4.32 ± 0.91	4.11 ± 0.90	4.58 ± 1.02
2.42×10^{17}	0.038 ± 0.004	0.023 ± 0.002	0.0083 ± 0.0008

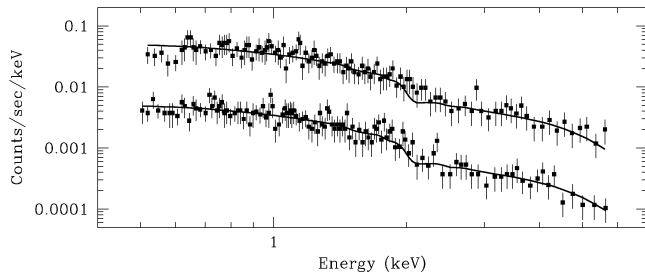


FIG. 4.—Two ACIS-S spectra that were simultaneously fitted with a power-law model ($\alpha = 0.60$; *solid lines*) including Galactic absorption of $N_{\text{H}} = 1.71 \times 10^{20}$ atoms cm^{-2} . Only data within 0.5–8 keV were included in the analysis. The fitting was performed on the original 1024 PI bins using Cash statistics in Sherpa. We rebinned the data to have a minimum of 10 counts bin^{-1} for the plotting purposes only. The upper data set, from observation ID 1711, is displayed in the original scale, while the lower data set, from observation ID 1712, was rescaled downward by $\times 10$ for clarity.

vation using filter F622W was used for direct comparisons with the X-ray jet profile, so the centroid of the quasar was determined by isolating the image diffraction spikes (Bahcall et al. 1995), fitting these with lines, and determining the intersection of the two lines (only two spikes were available from this image). Spatial distortions were corrected using polynomial coefficients given by Holtzman et al. (1995). The optical profile was obtained using the same method as used for the X-ray profile and is also shown in Figure 2. An offset of $0''.22$ was found between the centroids of the first X-ray peak and the peak of knot A1 from the PC image. The positional uncertainty is dominated by systematic uncertainties in measurement of the quasar core, so this difference between the X-ray and optical positions of this bright knot are not likely to be significant. The optical emission of A1 is clearly extended along a position angle (P.A.) closely aligned to the overall P.A. of the jet (see Fig. 1); the profile is well fitted by a Gaussian with $\sigma = 0''.3$, which is consistent with the X-ray profile at the 2σ level.

Identifying the sources of the remaining X-ray emission is not quite so straightforward as for knot A1. Region b (the extended knot at $15''$ from the core) is not consistent with a single point source at knot B1 but is likely to be a blend of point sources at knots B1 and A2, a somewhat weaker knot in the *HST* image. There appears to be a discrete source of X-ray emission near the positions of knots D and H3. More data are needed to tell whether knots besides these—i.e., C1, C2, and C3—are also discrete sources of X-ray emission.

3. DISCUSSION

3.1. Morphology

The overall shape of the jet is quite similar in the optical and X-ray bands: there is distinct curvature and the lengths are about the same. The optical emission between the knots is $\geq 0''.5$ wide (Bahcall et al. 1995), and the X-ray emission is marginally consistent with this level of broadening. There are several important differences, however. Knot A1 is much more prominent in the X-ray data than in the optical image. Furthermore, the X-ray jet fades along the jet, while the optical knots have similar brightnesses. Röser et al. (2000) also noted this difference.

The X-ray emission from knot A1 is consistent with a point source, but we cannot yet exclude the possibility that it is as extended as the optical emission along the jet axis. The MERLIN map shows that this knot is similarly extended in the

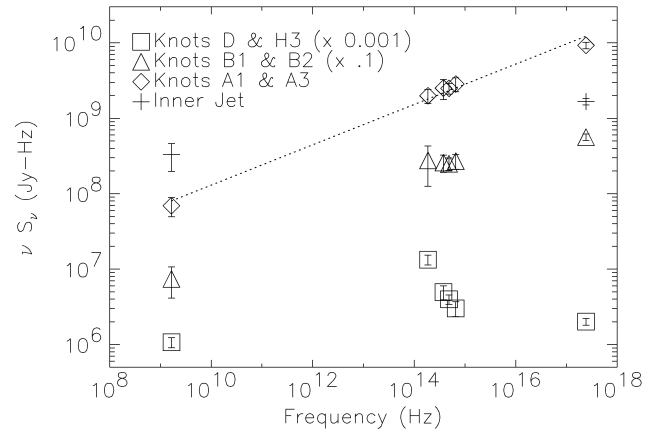


FIG. 5.—SEDs of the 3C 273 jet knots A1, B1/B2, D/H3, and the inner jet. The overall spectrum of knot A1 fits a simple power law, shown as the dashed line with a slope of 0.25, so the spectrum is consistent with a simple synchrotron model with a single power law distribution of electrons. For knot B1, however, the SED appears to flatten between the radio and optical bands; νS_{ν} still peaks in the X-ray band. A single synchrotron model does not fit the SED of the D/H3 region.

1.647 GHz band. The radio emission of the other knots is quite difficult to discern within the radio cocoon, giving rise to the impression that the bulk of the radio emission is physically distinct from the optical and X-ray emission regions. We find no significant X-ray emission from either extension (inner or outer; see Fig. 1), lending support to the interpretation that these are unrelated to the jet (Röser & Meisenheimer 1991).

3.2. Spectra

The overall SED for knot A1 (Fig. 5) appears to fit a simple synchrotron model, as suggested by Röser et al. (2000). Our estimate for the X-ray flux density is ~ 2 times higher, suggesting that the uncertainties derived from the *ROSAT* data were underestimated. Amazingly, the flux of this knot fits the overall slope of the SED (based on Table 2), 0.76 ± 0.02 , to within the uncertainties, even after extrapolating over several orders of magnitude in frequency. Furthermore, the spectral slope in the X-ray band is similar to that of the SED. Thus, the spectrum does not appear to break within the *Chandra* bandpass, which is consistent with the excellent spectral fit to the *Chandra* data. The luminosity of knot A1, 1.5×10^{43} ergs s^{-1} (for $q_0 = 0.5$ and $H_0 = 70$ km s^{-1} Mpc $^{-1}$), is about 40% of the total X-ray emission from jet, so, if the spectrum of knot A1 extends out to 100–200 keV with $\alpha = 0.6$, then its X-ray flux will dominate the total power of the jet. If the synchrotron break is above 5 keV, then $\gamma > 4 \times 10^7$ for the electrons, if one synchrotron model is to fit all the data. The magnetic field is 80 μG , based on minimum-energy arguments for nonrelativistic bulk motion. For a cylindrical emitting volume of the size defined by the optical emission, the SSC emission from knot A1 would be less than 0.1 nJy, well below the observed value.

Connecting the radio and optical/X-ray bands of the B1 SED requires a slight bend, consistent with the apparent flattening in the optical band. While the form of the electron energy distribution may not be a pure power law, no spectral cutoff is observed in the SED, so the electron energies may well reach energies comparable to those in knot A1. Röser et al. determined that SSC models of knot B1 would not give rise to such large X-ray fluxes, and we confirm this conclusion. As in knot

A1, νS_ν is much higher in the X-ray band than in the optical and radio bands. Because $\alpha < 1$ in the X-ray band, we do not yet know where the total powers of these knots peak.

Without detecting spectral cutoffs as observed in the first knot of the jet in PKS 0637–752 (Schwartz et al. 2000), we cannot tell whether there is a problem with the synchrotron model for knots A1 and B1 as found in that source. Similarly, the X-ray emission mechanism in the inner jet region is difficult to model without spectra from the radio and optical bands. Although there is no specific evidence that relativistic motion is required to explain the X-ray fluxes of the inner jet or knots A1 and B1, as in the model suggested by Tavecchio et al. (2000) and Celotti et al. (2001), this beaming model is a promising explanation for the X-ray fluxes of the weaker knots, so it could also provide an alternative to the synchrotron models

for knots A1 and B1. Thus, based on morphological similarities between the X-ray and optical images and considering that much of the jet power may be dissipated in the knots, we speculate that the knots are locations of internal shocks in a relativistic jet flow that is decelerating before equilibrating with the ambient medium. Alternatively, a helical jet structure would have regularly spaced inflection points where the local jet flow is close to the line of sight; beaming would be enhanced, giving rise to the observed knots.

q14

We thank Herman-Josef Röser for discussions about the *HST* data for which he was the principal investigator. We thank Tom Muxlow of Jodrell Bank for providing the MERLIN image. This research is funded in part by NASA contracts NAS8-38249, NAS8-39073, and SAO SV1-61010.

REFERENCES

- Albert, C. E., Blades, J. C., Morton, D. C., Lockman, F. J., Proulx, M., & Ferrarese, L. 1993, *ApJS*, 88, 81
- q15 Bahcall, J. N., Kirhakos, S., Schneider, D. P., Davis, R. J., Muxlow, T. W. B., Garrington, S. T., Conway, R. G., & Unwin, S. C. 1995, *ApJ*, 452, L91
- q16 Celotti, A., Ghisellini, G., & Chiaberge, M. 2001, *MNRAS*, submitted (astro-ph/0008021)
- Harris, D. E., & Stern, C. P. 1987, *ApJ*, 313, 136
- Holtzman, J. A., et al. 1995, *PASP*, 107, 156
- Röser, H.-J., & Meisenheimer, K. 1991, *A&A*, 252, 458
- Röser, H.-J., Meisenheimer, K., Neumann, M., Conway, R. G., & Perley, R. A. 2000, *A&A*, 360, 99
- Schwartz, D. A., et al. 2000, *ApJ*, 540, 69
- Tavecchio, F., Maraschi, L., Sambruna, R., & Urry, C. M. 2000, *ApJ*, 544, L23

q17

QUERIES TO THE AUTHOR

1 Au: ok to move the email address to footnote 1? I have added street addresses to footnotes 1 and 2, ok? Is there a street address I could add to footnote 3?

17 Au: “L69” changed to “69.”

2 Au: “distinct features which”: change to “distinct features that” ok, or would “distinct features, which” be better? Throughout the paper I have changed “which” to “that” or added a comma before “which” in order to distinguish between restrictive and nonrestrictive clauses, respectively. If the change I have selected is rejected, the other change will be inserted; pertinent queries are labeled “which/that.”

3 Au: ApJ style prefers single paragraph abstracts; ok to consolidate paragraphs here?

4 Au: “images with the Chandra”: change to “images from the Chandra” ok?

5 Au: “others, so was”: change to “others and so was” ok?

6 Au: please expand “ACIS”.

7 Au: “Because of pileup...affected by pileup”: this is redundant; please rephrase.

8 Au: you did not mention Fig. 4 in the text, but all figures must be cited. Is this the right place to cite it? If so, the figures will be renumbered so that they appear in order. If not, please indicate where you would like to cite Fig. 4.

9 Au: which/that

10 Au: have I expanded “NICMOS” correctly?

11 Au: which/that

12 Au: “either extensions”: change to “either extension” ok?

13 Au: a multiplication cross cannot be used in this situation, so I have spelled out “times,” ok?

14 Au: your manuscript comes out to more than four pages. Could you suggest any ways to shorten it?

15 Au: ApJ spells out all author names if fewer than nine.

16 Au: any update available?

The Astrophysical Journal

The University of Chicago Press
5608 Stony Island Avenue
Chicago, IL 60637
FAX (773) 753-0827

NO REPRINTS DESIRED

2000 PAGE CHARGE / REPRINT ORDER FORM

(please keep a copy of this document for your records)

AUTHORS Please return this form immediately **even if no reprints are desired**. The form on the reverse side should be used to calculate page charges, color printing costs, and reprint costs. This form should be used to order reprints and allocate cost of page charges, color printing costs, and reprints. Payment by check, wire transfer, Visa, or MasterCard is accepted for all orders not accompanied by an institutional purchase order or purchase order number. Reprints ordered through an institution will not be processed without a purchase order number. **Make checks and purchase orders payable to The University of Chicago Press.** All purchase orders MUST include the following: journal name and date of issue, authors' names, title of article, and number of reprints ordered. Billing questions may be directed to Cindy Garrett, Billing Coordinator (tel. (773) 753-8028; fax (773) 753-0827; email cgarrett@journals.uchicago.edu).

THE ASTROPHYSICAL JOURNAL PART 1 LETTERS SUPPLEMENT VOL. _____ NO. _____ ISSUE _____

TITLE OF ARTICLE _____

AUTHOR NAME _____

ESTIMATED NUMBER OF PAGES _____ MANUSCRIPT # _____ NUMBER OF COLOR FIGURES TO APPEAR IN PRINT _____

PAGE CHARGES

Invoice(s) to be sent to the following address(es)

_____ % to be paid by

_____ % to be paid by

MAKE CHECKS & PURCHASE ORDERS PAYABLE TO

The University of Chicago Press. All orders must be accompanied by one of three payment options:

- 1) Institutional Purchase Order No. _____
Purchase Order attached to come
- 2) Check or Money Order for total charges is attached **OR**
- 3) Please charge to VISA MasterCard

Card Number _____

Expiration date _____

Signature _____

Phone number _____

Contact _____

Tel/Fax/email _____

Signature of Administrative Official _____

REPRINT CHARGES

Please send the following quantity _____

without covers with covers

Ship reprints to

Send invoices to

_____ % to be paid by

Payment options

- 1) Institutional Purchase Order No. _____
Purchase Order attached to come
- 2) Check Wire transfer VISA **OR** MasterCard
- 3) Credit card to be used as: proof of payment **OR** payment

Card Number _____

Expiration Date _____

Signature _____

Phone number _____

MAKE CHECKS & PURCHASE ORDERS PAYABLE TO

The University of Chicago Press. All orders must be accompanied by one of three payment options:

- 1) Institutional Purchase Order No. _____
Purchase Order attached to come
- 2) Check or Money Order for total charges is attached **OR**
- 3) Please charge to VISA MasterCard

Card Number _____

Expiration date _____

Signature _____

Phone number _____

Contact _____

Tel/Fax/email _____

Signature of Administrative Official _____

Please send the following quantity _____

without covers with covers

Ship reprints to

Send invoices to

_____ % to be paid by

Payment options

- 1) Institutional Purchase Order No. _____
Purchase Order attached to come
- 2) Check Wire transfer VISA **OR** MasterCard
- 3) Credit card to be used as: proof of payment **OR** payment

Card Number _____

Expiration date _____

Signature _____

Phone number _____

2000 PAGE CHARGES /REPRINT PRICES

AUTHORS This form should be used to calculate page charges, color printing costs, and reprint costs. Payment by check, Money Order, Visa, or MasterCard is required with all orders not accompanied by an institutional purchase order or purchase order number. **Make checks and purchase orders payable to The University of Chicago Press.**

PAGE CHARGES for ApJ Part 1, ApJ Part 2 (Letters), and ApJ Supplement

Type of Charge	Charge
ApJ Part 1 or ApJ Supplement Electronic manuscript	\$115 per page
ApJ Part 1 or ApJ Supplement Paper manuscript	\$130 per page
<i>ApJ Part 2 (Letters) paper or electronic manuscripts</i>	<i>\$155 per page</i>
Extended data table to appear in the electronic edition only	\$115 per table
Color figure(s) in the print edition	\$600 per figure + \$150 per each additional color figure
Author alterations	\$6.00 per change

REPRINT CHARGES

Please use the following chart to determine the cost of your reprints. Without proof of payment, reprint orders will not be processed. No free reprints are provided. Reprints may not be ordered when page charges have been waived. The minimum order is **50** copies. Please indicate the quantity desired by each author along with shipping and billing addresses in the spaces provided. Please allow 4-6 weeks after publication for delivery. Shipping costs are included in these reprint prices. Faster delivery can be arranged at the author's expense; please contact the billing coordinator.

	50	100	150	200	ADD'L 50
# OF PAGES					
1-4	\$77	\$87	\$98	\$109	\$20
5-8	\$109	\$119	\$130	\$142	\$30
9-12	\$142	\$152	\$163	\$174	\$40
13-16	\$174	\$184	\$195	\$207	\$50
17-20	\$207	\$217	\$229	\$239	\$61
21-24	\$239	\$249	\$261	\$272	\$68
25-28*	\$272	\$282	\$294	\$304	\$78
COVERS	\$77	\$87	\$98	\$109	\$20

*For articles with a larger number of pages, combine rates (e.g., 36 pages = 28 + 8, 50 reprints will cost \$272+ \$109 = \$381).

- If more than two institutions are paying page charges, please submit information on a separate sheet attached to this form.
- If page charges are to be paid from funds with a specific expiration date and early billing is necessary, please request advance billing from the billing coordinator at least 30 days prior to the expiration date. The billing amount will be based on an estimate of paper length. Extensive additions or alterations to any paper that is prebilled could result in higher costs, depending on the nature of the changes.

PUBLICATION AGREEMENT
American Astronomical Society

Date: _____ (must be filled in)

To: (Name) _____
(Address) _____
(City, State) _____
(Country) _____

Manuscript #: _____ (must be filled in)

Dear Colleague:

With regard to your original and previously unpublished paper entitled:

written by you and _____

which has been accepted for publication in our journal, the following terms are submitted for your consideration. If these terms are satisfactory, please sign below and return this agreement to us. We cannot publish your paper without this approval.

Copyright Assignment: Because the Society, acting through the University of Chicago Press, is undertaking to publish this paper, and because you desire to have this paper so published, you grant and assign the entire copyright for this paper exclusively to the Society. The copyright consists of all rights protected by the copyright laws of the United States and of all foreign countries, in all languages and forms of communication.

The Society, in turn, grants to you the non-exclusive right of republication, subject only to your giving appropriate credit to the Journal. To protect the copyright in this paper, the original copyright notice as it appears in the Journal should be included in the credit.

Compensation and Subsidiary Rights: It is understood that you will receive no monetary compensation from the Society for the assignment of copyright and publication of the paper. Please note, however, that you may grant or deny requests to reprint this paper in books or journals, and you may retain all fees from such reprinting. We will forward such requests to you.

Who Should Sign: The agreement should be signed by at least one of the authors (who agrees to inform the others, if any) or, in the case of a work made for hire, by the employer.

An author who is a U.S. Government officer or employee and who prepared the paper as part of his or her official duties does not own any copyright in it. If at least one of the authors is not in this category, that author should sign below. If all the authors are in this category, please return this form unsigned.

FOR THE AMERICAN ASTRONOMICAL SOCIETY:


Robert C. Kennicutt, Jr., Editor-in-Chief


A. Dalgarno, Letters Editor

ACCEPTED AND APPROVED FOR THE AUTHOR(S)

Author's signature

DATE: _____